

Monte Carlo modeling of organic polymer light-emitting devices on flexible plastic substrates

Shu-jen Lee^{a,b}, Aldo Badano^c, and Jerzy Kanicki^{*a,b}

^aOrganic and Molecular Electronics Laboratory, Department of Electrical Engineering and Computer Science, University of Michigan, Ann Arbor, MI 48109

^bMacromolecular Sci. & Eng. Center, University of Michigan, Ann Arbor, MI 48109

^cCenter for Devices and Radiological Health, Food & Drug Administration, Rockville, MD 20857

ABSTRACT

A Monte Carlo method for modeling the light transport phenomena in organic polymer light-emitting devices (PLEDs) is reported. In this simulation we assumed a point light source having photon emission spectrum represented by the photoluminescence (PL) spectrum of the organic polymers. This method describes the fate of photons through multiple scattering events determined by the wavelength-dependent material optical properties in a 3-D Cartesian geometry, thus considering the effects of refraction at different interfaces, back-reflection from the cathode, interference effect in the ITO thin film, and absorption within the polymer layers. We apply this method to analyze the wavelength output distribution and extraction efficiency. We found that the simulated light emission spectra of the green and red light-emitting devices are very similar to the measured PL spectra, suggesting that the light transport phenomena do not change the energy distribution significantly. We also established that the calculated extraction efficiency for the red ($\eta_{ext}=19.5\%$) and green ($\eta_{ext}=19.9\%$) PLEDs are approximately the same. We further investigated the light emission angular distribution of the PLEDs, and found that the simulated angular distribution shows better agreement with the experimental data than previously used models that rely on standard refraction theory at one interface.

Keywords: Organic polymer light-emitting devices, light transport phenomena, extraction efficiency, angular distribution, Monte Carlo method

1. INTRODUCTION

The external quantum efficiency of the PLEDs are limited by four major losses: the charge injection and charge transport process, the electron and hole radiative recombination process, the photo-luminescent efficiency, and the light extraction efficiency. It is estimated that the light extraction efficiency is about one-fifth of the total internally generated light by applying a standard refraction theory.¹ Later, several models have been also used for modeling organic light emitting devices, such as half-space optical model,² one-dimensional ray-tracing model,³ and quantum mechanical micro cavity model.^{4,5} The method that we present in this paper is based on a Monte Carlo approach.⁶ This statistical method has the flexibility for modeling events such as absorption, waveguiding, scattering, extraction, and trapping happening in the devices. Possible reporting options from this program include the angular and spectral distributions of the emitted photons, the point-spread function, the specular and diffuse reflection coefficients, and a summary of scattering events statistics, thus obtaining important design parameters for achieving full-color efficient PLEDs for flat-panel display applications. The unique advantage of this method is its ability to model bulk absorption events, thin film coatings, and rough surfaces while keeping track of the photon polarization state.

* Contact: Jerzy Kanicki; kanicki@eecs.umich.edu; <http://www.eecs.umich.edu/omelab/>; phone: 1-734-936-0972; fax: 1-734-615-2843; Organic & Molecular Electronics Lab.; 1049 BIRB, 2360 Bonisteel Blvd., Ann Arbor, MI 48109

2. EXPERIMENT AND SIMULATION METHOD

A. Experiment

The organic polymer light emitting device (PLED) structure used for the angular distribution measurement and the optical modeling is showed in Fig. 1. The PLEDs were fabricated on the 2" by 2" plastic substrates coated with eight patterned ITO fingers. The ITO fingers were used as transparent anodes in PLEDs with a sheet resistance of $\sim 10 \text{ ohm}/\square$ and a transparency higher than 80% over the visible range (400 – 800 nm). The ITO-covered substrates were cleaned in an ultrasonic bath of isopropanol for 20 minutes and exposed to UV-ozone for 10 minutes before polymer spin coating. First, a hole-transport layer (HTL, $\sim 700 \text{ \AA}$), poly(3,4-ethylenedioxythiophene)-poly(styrene sulfonate) (PEDOT-PSS), was spin-coated from the solution and followed by thermal curing at 90°C for 20 minutes. Then, an emissive layer (EL, $\sim 1000 \text{ \AA}$) was spin-coated from the solution in xylene and was followed by thermal curing at 90°C for 1 hour. A calcium cathode ($\sim 400 \text{ \AA}$) and then an aluminum cathode ($\sim 2000 \text{ \AA}$) as a capping layer were evaporated through shadow masks in a thermal evaporation system under a high vacuum ($\sim 10^{-7}$ torr). This gives a square metal film that overlaps with the ITO fingers to define eight $0.1'' \times 0.1''$ PLEDs. The device was then mounted on a goniometer stage with an angular precision of $\pm 1^\circ$ for the angular distribution measurements. The detector used for recording the light emission was a CCD spectrometer with an integrating sphere at the front exit. The detector was calibrated with a tungsten filament lamp standard with known spectral irradiance ($\text{W}/\text{cm}^2/\text{nm}$), so the spectral radiant intensity ($\text{W}/\text{sr}/\text{nm}$) of the PLEDs could be accurately measured at the given angle. The CIE (Commission Internationale de l'Éclairage) standard condition B⁷ for the measurement of the averaged LED intensity was used for the measurement of the PLED intensity. The distance between the PLED and integrating sphere with a circular entrance aperture having an area of 1 cm^2 was 10 cm, thus defining the measuring solid angle, the area of the circular aperture divided by the square of the distance, as 0.01 sr . Since the size of the emitting area ($\sim 0.0645 \text{ cm}^2$) of the PLED and of the receiving surface of the detector ($\sim 1 \text{ cm}^2$) are small enough to be insignificant compared to the distance between the two ($\sim 10 \text{ cm}$), the point source approximation of the CIE condition B is satisfied.⁷ The radiant intensity was then collected as a function of the external viewing angle as shown in Fig. 2. We then normalized the radiant intensity with respect to its value at the angle normal to the plane of the PLED.

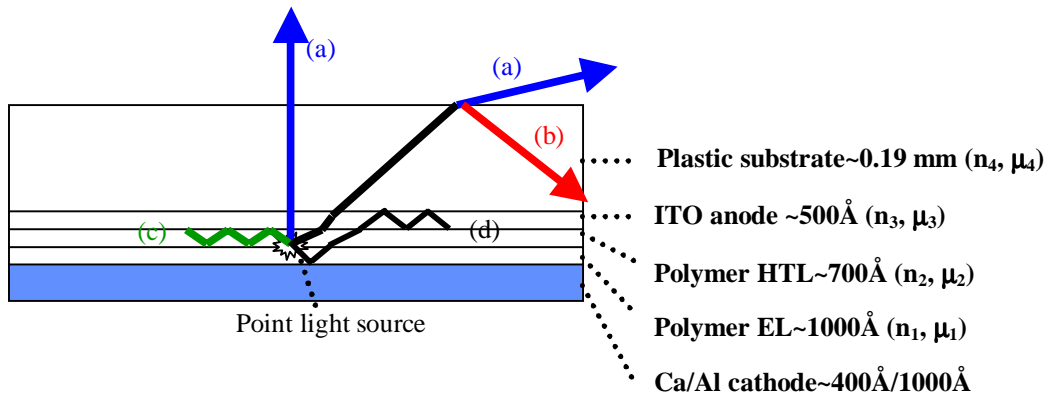


Figure 1. Schematic representation of the device structure used in the angular distribution measurement and Monte Carlo simulation. A point light source was specified at the interface between the polymer hole transport layer and polymer emissive layer.

B. Optical modeling

We used DETECT-II, a Monte Carlo method for the simulation of light transport processes in emissive structures.^{6,8} We simulated the PLEDs by generating photons according to a distribution function describing the nature of the light emission. The light source generated in the amorphous polymer emissive layer was considered to be an isotropic point situated in the center of the device interface between HTL and EL. To obtain an isotropic distribution, the three directional cosines (C_x, C_y, C_z) that define the photon direction in a Cartesian coordinate system were sampled according to

$$C_x = \sqrt{1 - \xi_1^2} \sin 2\pi\xi_2 \quad \text{Eq. (1)}$$

$$C_y = \sqrt{1 - \xi_1^2} \cos 2\pi\xi_2 \quad \text{Eq. (2)}$$

$$C_z = \xi_2 \quad \text{Eq. (3)}$$

where ξ_1 and ξ_2 are random deviates uniformly sampled in [0,1). The energy distribution of the light source is defined by a table corresponding to the photo-luminescence spectra of the light-emitting layer. The initial photon polarization vector was sampled uniformly in the 4π space, therefore assuming unpolarized light emission. The light path of the photons was determined by the interaction of the light quanta with optical boundaries, described by the Snell's law, and by the events that may result in absorption. The light quanta would be reflected or transmitted when going from medium 1 to medium 2 at an optical boundary. We then used the Fresnel's equations to calculate the transmission and reflection coefficients depending on the surface type and material properties,⁹ and interpreted these coefficients as probabilities of refraction and reflection. When the film thickness is comparable to the photon wavelength, we used the modified Fresnel coefficients to describe the interference effect of optical thin films.

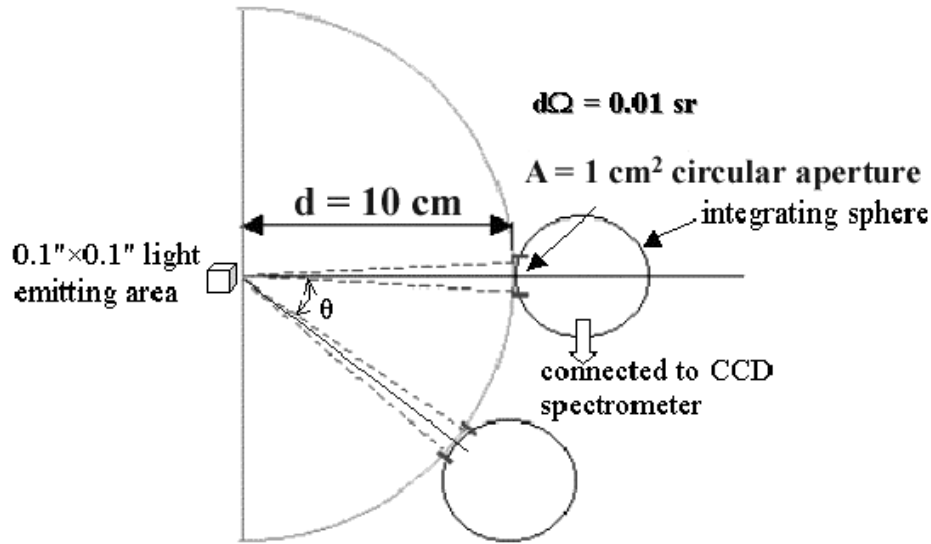


Figure 2. Schematic representation of the setup used for angular distribution measurement. The CIE (Commission Internationale de l'Éclairage) standard condition B for the measurement of the averaged LED intensity was used for measuring the PLED light intensity.

Bulk absorption is determined by sampling the probability of a photon being absorbed after a path of length l by the exponential law

$$P(l) = 1 - e^{-\mu_{ab}(\lambda)l} \quad \text{Eq. (4)}$$

where $\mu_{ab}(\lambda)$ is the wavelength dependent linear absorption coefficients. The simulation outcome was calculated by a statistical average of about 10^7 photon histories.

The external quantum efficiency (η_e) of the PLEDs are limited by four major losses: the charge injection and charge transport efficiency (η_{inj}), the efficiency of the formation of the radiative excited electron hole pairs (η_{rad}), the photo-luminescent efficiency (η_{PL}), and the photon extraction efficiency (η_{ext}), therefore it could be written as

$$\eta_e = \eta_{inj} \eta_{rad} \eta_{PL} \eta_{ext} \quad \text{Eq. (5)}$$

The product $\eta_{inj} \eta_{rad} \eta_{PL}$ defines the intrinsic limitation for the external quantum efficiency of PLEDs. We define the photon extraction efficiency as the fraction of the light output of the internally generated light. As shown in Fig. 1, the internally generated light could possibly exit through the front plate η_{ext} (a), waveguide within the device structure

and exit through the device edges η_{wav} (b), be absorbed within the polymer layers η_{abs} (c), and be trapped in the ITO optical thin film η_t (d). The photon extraction efficiency could then be written as:

$$\eta_{ext} = 1 - \eta_{wav} - \eta_{abs} - \eta_t \quad \text{Eq. (6)}$$

In this simulation, we neglect the light leakage through the cathode side, and the photo-luminescence quenching due to polymer composition variations and the presence of carrier flow within the PLEDs. Electric field induced photoluminescence quenching in conjugated polymers is experimentally confirmed by our group, but cannot be implemented easily in this calculation.¹⁰ It should be noted that this PL quenching is not important at the PLED operating point.

3. RESULTS AND DISCUSSION

Fig. 3 shows the variation of refractive indices and the absorption coefficients with photon wavelength of the red and green polymers used in the simulation. The absorption coefficients were obtained by a combination of the UV-vis absorption spectroscopy and the photothermal deflection spectroscopy.¹¹ The data from the UV-vis absorption spectroscopy was only to be trusted down to about $5 \times 10^3 \text{ cm}^{-1}$ and was uncertain at low values because of the unknown exact reflectivity of the polymer films. The absorption coefficients of these two measurements agree well with each other near the principal $\pi - \pi^*$ absorption peak, therefore the absorption coefficients are obtained accurately by a combination of those two methods. The spectrometric ellipsometer was used to measure the refractive indices of the red and green light emitting polymers, the hole transport layer, and ITO thin film. The refractive index of the 0.19 mm thick transparent plastic substrate was 1.5.

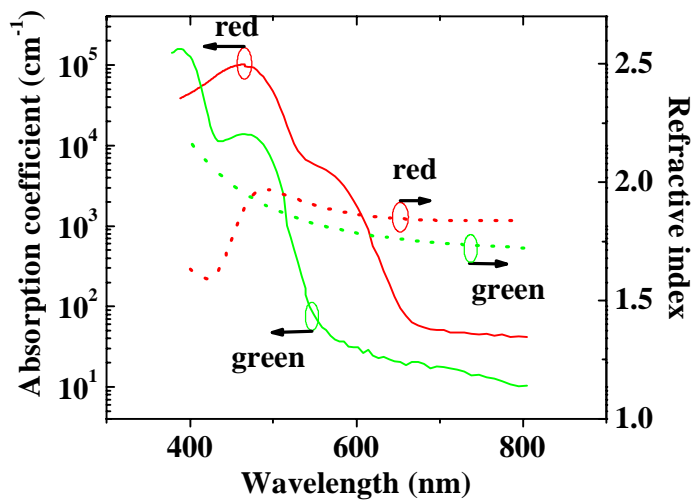


Figure 3. Refractive indices and absorption coefficients of the red and green polymers used in this work.

In this analysis, we used the photo-luminescent spectra of the green and red polymers as the input light source spectra as shown in Fig. 4. The input photons go through a series of events, such as refraction, reflection, and absorption, and finally exit out or are killed in the device. The red and green output spectra after the light transport process in the PLEDs are the simulated spectra as shown in Fig. 4. We observe that the simulated spectra do not change significantly when compared with light source spectra of our red and green PLEDs, indicating that the light transport process does not change the energy distribution of the light significantly. For some of our reported cases,⁶ the weight of the absorption of the polymer film is higher in the shorter wavelength range, therefore the simulated spectrum would shift slightly toward the longer wavelength region. For the light emitting polymers with significant overlap between their absorption and photo-luminescent spectra, the polymer film will then act like a filter of their electro-luminescent spectra, thus shifting the whole spectra to longer wavelengths.

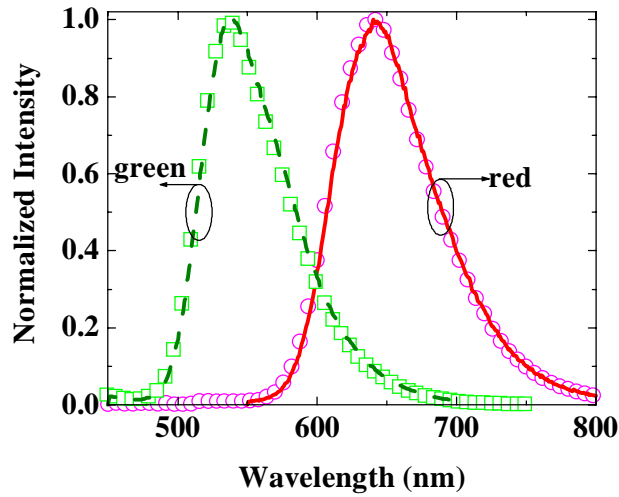


Figure 4. Measured photo-luminescent (\square open square) and simulated (---- dashed line) light emission spectra of the green PLED, and measured photo-luminescent (O open circle) and simulated (— solid line) light emission spectra of the red PLEDs.

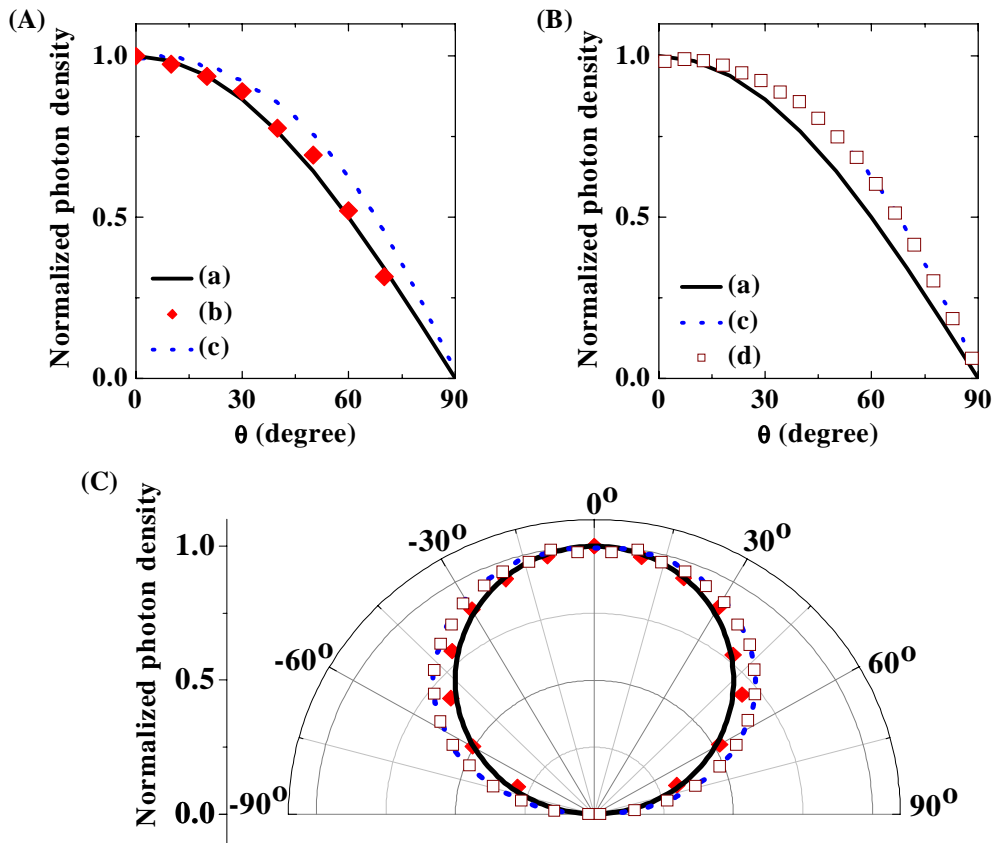


Figure 5. Experimental and simulated angular distribution of the PLEDs light emission: (A) Comparisons among (a) Lambertian behavior (— solid line), (b) experimental data (\blacklozenge filled diamond), and (c) simple model based on standard refraction theory (.... dotted line), (B) comparisons among (a), (c), and (d) simulated result with one refraction and back-reflection (\square open square), and (C) Comparisons among (a), (b), (c), and (d) in polar coordinate.

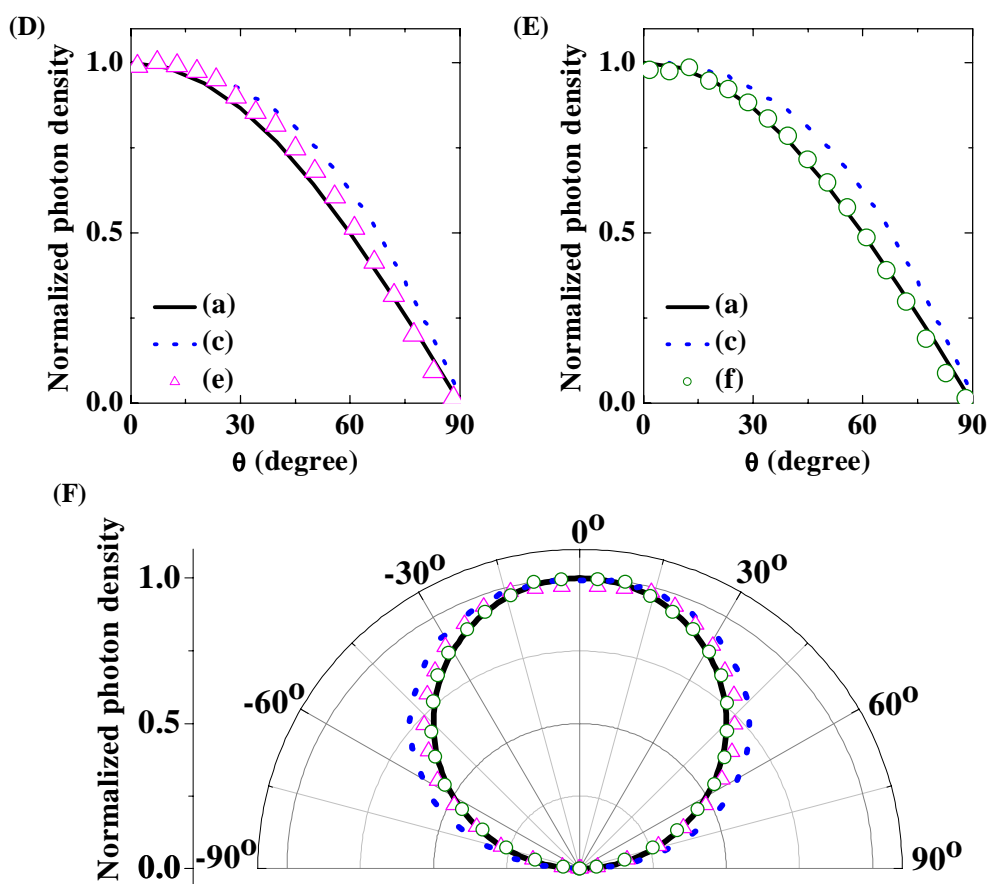


Figure 6. Experimental and simulated angular distribution of the PLEDs light emission: (D) Comparisons among (a) Lambertian behavior (— solid line), (c) simple model based on standard refraction theory (.... dotted line), and (e) simulated result with back reflection, multiple refractions, and polymer absorption (Δ triangle), (E) Comparisons among (a), (c), and (f) simulated result with back-reflection, multiple refractions, polymer absorption, and interference effect in ITO thin film (O circle), and (F) Comparisons among (a), (c), (e), and (f) in polar coordinate.

Fig. 5(C) shows the polar plot of the angular distribution of a Lambertian light source (a), experimental angular distribution of a red polymer device (b), simulated angular distribution with refraction between the polymer emissive layer and air (c), and simulated angular distribution with refraction at the interface and back reflection from the cathode (d). Both the angular distribution results of the experimental and simulated data with same device structure and material properties are similar for green and red PLEDs. Therefore, we will mainly discuss the red polymer device in this article. We plot our experimental and simulated data in both polar and one-dimensional plots for the ease of clarification of different data. As can be seen in Fig. 5(A) and Fig. 5(C), the experimental angular distribution of our red polymer device is very close to that of a Lambertian light source, which agrees with published results by other groups.²⁻⁵ When we apply the Monte Carlo method on a simple device structure with just refraction between the polymer emissive layer and air, a broader emission pattern when compared with the experimental result is obtained as shown in Fig. 5(B) and Fig. 5(C). We compared this emission pattern with the model proposed by Greenham et. al¹, and found that our results of a simple device structure show excellent agreement with Greenham's model. However, this simple model does not take the polymer absorption, back-reflection from the cathode, and the light trapping in the ITO thin film into considerations. A discrepancy between the simulated and experimental results exists. As can be seen in Fig. 6(D) and Fig. 6(F), the back-reflection from the cathode does not change output angular distribution significantly when compared with the simple model. We further simulated the case with multiple refractions, back-reflection, and polymer absorption, and without ITO thin film represented by curve (e) in Fig. 6(D) and 6(F). In this case, the simulated result shows significant narrower

angular distribution when compared with the simple model that neglects the absorption and multiple refractions. In the last case, we take the multiple refractions, the back-reflection from the cathode, the polymer absorption, and the interference effect in the ITO thin film into considerations represented by curve (f) in Fig. 6(E) and 6(F), and we find excellent agreement between the simulated and experimental results. As can be seen in the previous cases, the refraction at different interfaces contributes significantly to the Lambertian behavior of the PLEDs when assuming an isotropic emitting center. The interference effect of the ITO thin film and the polymer absorption also contribute to the Lambertian behavior of the PLEDs, while the back reflection from the cathode does not have a significant effect.

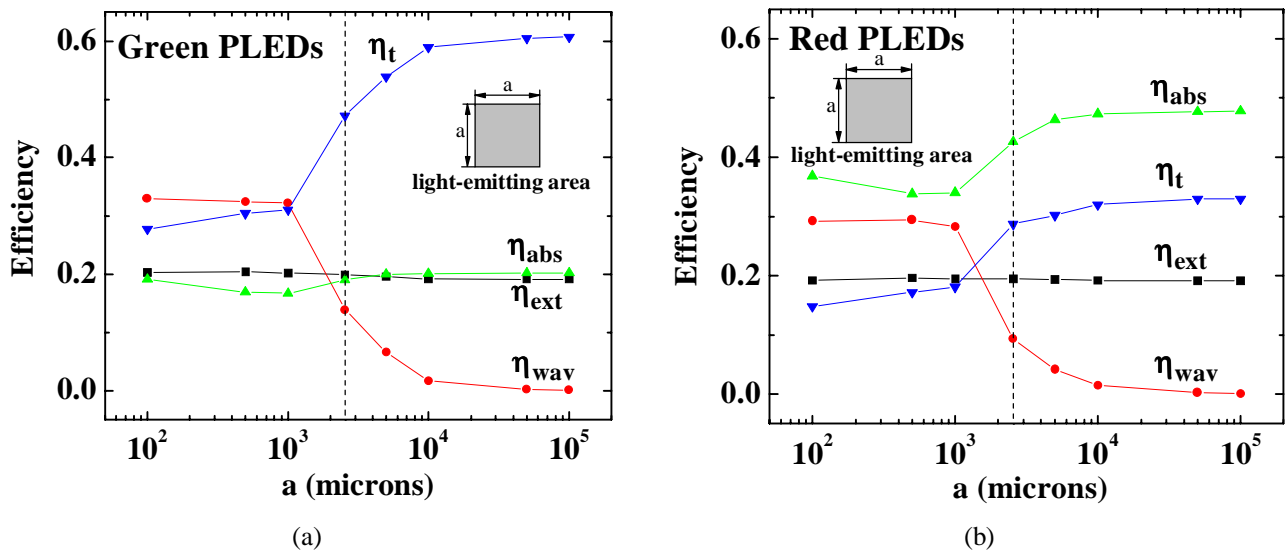


Figure 7. The photon extraction η_{ext} , waveguiding η_{wav} , absorption η_{abs} , and trapping η_t parts of the green (a) and red (b) PLEDs with different device sizes. The device has a square light emitting area, and its device cross section is shown in Fig. 1. The x-axis represents the length of a side.

We have applied this method to calculate the extraction efficiency for the green and red PLEDs with the device configuration shown in Fig. 1, and we have found that the photon extraction η_{ext} , waveguiding η_{wav} , absorption η_{abs} , and trapping η_t parts are 0.20, 0.14, 0.19, and 0.47 for $0.1'' \times 0.1''$ green PLED and 0.20, 0.09, 0.43, and 0.29, for $0.1'' \times 0.1''$ red PLED respectively. Since the refractive index at 633 nm for the green and red polymers is 1.78 and 1.85, respectively, the photon extraction efficiency is estimated to be 0.16 and 0.15, respectively, by using a standard refraction theory at one interface. The photon extraction efficiencies obtained from our simulation are slightly larger than those obtained by standard refraction theory at one interface because we consider the multiple refractions. As can be seen in Fig. 7, the calculated extraction efficiencies for both green and red PLEDs are approximately the same, while the waveguiding part decreases significantly from $\sim 30\%$ to $\sim 0\%$ when PLED size increases from 10^2 to 10^5 microns. The decrease in waveguiding is due to the increase of absorption in the polymer layers and trapping in the ITO thin-film when PLED size increases.

4. CONCLUSIONS

We have demonstrated a light transport Monte Carlo code for modeling the real PLEDs structure. This method takes the absorption in the polymer, the back-reflection from the cathode, and the interference effect of the optically thin ITO film into account. We show that the simulated output spectra are similar to the experimental light source spectra, suggesting the light transport process does not change the light energy distribution significantly. We also demonstrate that the simulated output angular distribution shows better agreement with the experimental angular distribution than the predictions of a simpler model that relies on standard refraction theory. Finally, we show that red and green polymer

PLEDs have similar simulated photon extraction efficiency and angular distribution of the light emission. In the future, we plan to expand this method to model a variety of PLED display structures.

ACKNOWLEDGMENTS

This research was supported by NIH grant. The authors would like to thank Dr. Sandrine Martin and Yongtaek Hong for useful discussions.

REFERENCES

-
- 1 N. C. Greenham, R. H. Friend, and D. D. C. Bradley, *Adv. Mater.*, **6(6)**, 491 (1994).
 - 2 J. S. Kim, P. K. H. Ho, N. C. Greenham, and R. H. Friend, *J. Appl. Phys.*, **88(2)**, 1073 (2000).
 - 3 S. Moller and S. R. Forrest, *J. Appl. Phys.*, **91(5)**, 3324 (2002).
 - 4 C. F. Madigan, M. H. Lu, and J. C. Sturm, *Appl. Phys. Lett.*, **76(13)**, 1650 (2000).
 - 5 V. Bulović, V. B. Khalfin, G. Gu, P. E. Burrows, D. Z. Garbuzov, and S. R. Forrest, *Phys. Rev. B*, **58**, 3730 (1998).
 - 6 A. Badano and J. Kanicki, *J. Appl. Phys.*, **90(4)**, 1827 (2001).
 - 7 Commission Internationale de l'Éclairage, *Measurement of LEDs*, Publication CIE **127**, 14 (1997).
 - 8 A. Badano, Ph.D. thesis, University of Michigan, Ann Arbor, MI (1999).
 - 9 M. Born and E. Wolf, *Principles of Optics*, 3rd ed., Pergamon, New York (1965).
 - 1 0 S. J. Lee and J. Kanicki, unpublished results.
 - 1 1 C. H. Seager and C. E. Land, *Appl. Phys. Lett.*, **45**, 395 (1984).